

Radio Supernovae

By KURT W. WEILER,¹ SCHUYLER D. VAN DYK,¹
RICHARD A. SRAMEK,¹ AND NINO PANAGIA¹

¹Remote Sensing Division, Code 7215, Naval Research Laboratory, Washington, DC 20375-5351, USA

²National Radio Astronomy Observatory, P.O. Box O, Socorro, NM 87801, USA

³Space Telescope Science Institute, 3700 San Martin Drive, Baltimore, MD 21218, USA

Radio observations have shown that some supernovae are powerful radio emitters which increase rapidly in brightness to radio luminosities which are hundreds to thousands of times greater than even the brightest known supernova remnant, Cas A. They then fade over a period of weeks, months, or years. This radio emission has been found to provide important information about the nature of the progenitor stars, their mass loss rates, and the circumstellar material surrounding them. RSN observations may also offer the possibility of extragalactic distance measurements and the presence of radio emission appears to be indicator of strong x-ray emission and late time optical emission.

1. Introduction

Detailed studies of radio emission from supernovae have now been carried out for over a decade with SN1979C providing the first example of a radio supernova (RSN) which could be detected and monitored in detail over a lengthy time span. The monitoring of the radio emission from SN1979C is still continuing. Additionally, in the intervening 13 years a number of other SNe have been detected at radio wavelengths and these are listed in Table 1. This list is complete at the present time. However, it is limited to objects which show most or all of the RSN properties which are listed in Section 5, and in practice includes only “young” SNe occurring since the first radio detection of an SN, SN1970G, by Gottesman et al. (1972). This restricts our discussion to a relatively well defined group of objects which can be systematically discussed and classified. The so-called intermediate age RSNe – SN1961V (Branch & Cowan 1985, Cowan, Henry, & Branch 1988), SN1950B (Cowan & Branch 1985), and SN1957D (Cowan & Branch 1985) are discussed separately in Section 4 and the compact radio emitters in M82 (Kronberg & Sramek 1985) are not discussed because of their unusual and poorly understood nature. The two brightest SNe of the past decade, SN1987A and SN1993J, are discussed only in a very limited fashion since SN1987A was a very unusual and atypical SN in all wavelength bands and SN1993J is discussed elsewhere in this volume (Van Dyk et al. 1993). We provide only an overview here; for more detailed information consult the references listed in Table 1. Weiler et al. (1986), Weiler & Sramek (1988), and Sramek & Weiler (1990) also provide an overview of the subject.

2. Type I Radio Supernovae

2.1. *Type Ia Supernovae*

No Type Ia SN has ever been observed to be a RSN, even in cases with quite early observations (SN1981B and SN1980N; Weiler et al. 1986) or a very small distance (SN1972E; (Cowan & Branch 1982, Branch & Cowan 1985, Weiler et al. 1989). This implies that Type Ia are in systems which contain very little circumstellar material at the time of the

TABLE 1. Known RSNe

SN	Optical Type	Refs.
1983N	Ib	1,2
1984L	Ib	2,3
1990B	Ic	4
1970G	II	2
1978K	II	5
1979C	II	2,6,7,8,9
Mkn 297A	II	10,11
1980K	II	2,12
1981K	II	2,13
1986J	II	14
1987A	II	15,16,17
1988Z	II	18
1993J	II	19

explosion. For example, the upper limit to the mass loss rate for SN1981B is less than one third of that measured for Type Ib supernovae SN1983N and SN1984L (see Weiler et al. 1986 and references therein). This represents a major difference between the two Type I SN subclasses and confirms the suggestion that they originate from systems of very different masses.

2.2. Type Ib/c Supernovae

2.2.1. SN1983N

When the Type Ib supernova SN1983N was discovered in NGC5236 (M83) in the optical, radio observations were started immediately and, due to good fortune in obtaining very early measurements, SN1983N was detected at 6 cm already 11 days before optical maximum. The radio emission evolved extremely rapidly (Sramek, Panagia, & Weiler 1984) and, while the Type II supernovae SN1979C and SN1980K have remained detectable in the radio for many years, in less than one year SN1983N could no longer be detected to the sensitivity limit of the VLA. In addition to the very rapid rise and decline of its radio emission, SN1983N also showed an optically thin spectral index which was significantly steeper ($\alpha \sim -1$) than that found for SN1979C and SN1980K. The radio light curves for SN1983N, which are typical for Type Ib supernovae, are shown in Figure 1.

2.2.2. SN1984L

A second Type Ib supernova, SN1984L, has been detected with the VLA and, to the limit of the somewhat sparse data set available, appears to behave in a fashion very similar to SN1983N. The steeper spectral index and rapid rate of decline of the centimeter flux density after maximum are both apparent, again demonstrating that Type Ib SNe are a class which is distinct in its radio properties from either the Type II or the Type Ia supernovae. The results for SN1984L are discussed in more detail in Panagia, Sramek, & Weiler (1986) and Weiler et al. (1986).

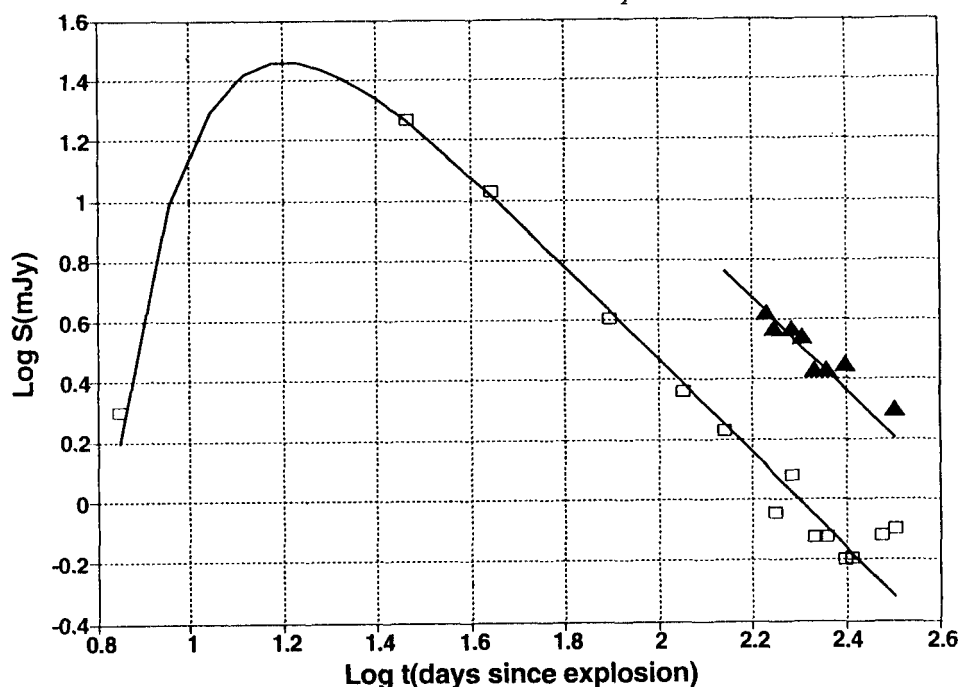


FIGURE 1. Radio light curves at 6 cm (squares) and 20 cm (triangles) wavelength for the Type Ib supernova SN1983N in NGC5236 (M83) (From Weiler et al. 1986).

2.2.3. *SN1990B*

Recently, the Type Ic supernova SN1990B has been detected in the radio. Although weak and distant, its radio light curves and parameters agree well with the values previously found for SN1983N and SN1984L. It is described in detail by Van Dyk et al. (1993a).

3. Type II Radio Supernovae

3.1. *SN1970G*

SN1970G was first detected in the radio by Gottesman et al. (1972) followed by more extended study by Allen et al. (1976). The available early radio data have been discussed by Weiler et al. (1986). More recently, the supernova has been recovered in the radio by Cowan, Goss, & Sramek (1991). Although the data is very poor, the general behavior of the radio emission from SN1970G resembles that from the better studied “normal” Type II RSNe such as SN1979C and SN1980K.

3.2. *SN1978K*

SN1978K has only recently been discovered at radio wavelengths by Ryder et al. (1993). Although the available radio data are still quite sparse, the RSN appears to behave in both its temporal and spectral characteristics like a Type II supernova. In particular, its optical, x-ray, and radio properties all indicate that it is probably an example of a “peculiar” Type II RSN like SN1986J and SN1988Z. Although much of the important turn-on phase of the radio emission has been missed, making it difficult to determine model parameters, future observations will certainly allow rough estimates of the properties of the presupernova stellar system to be made.

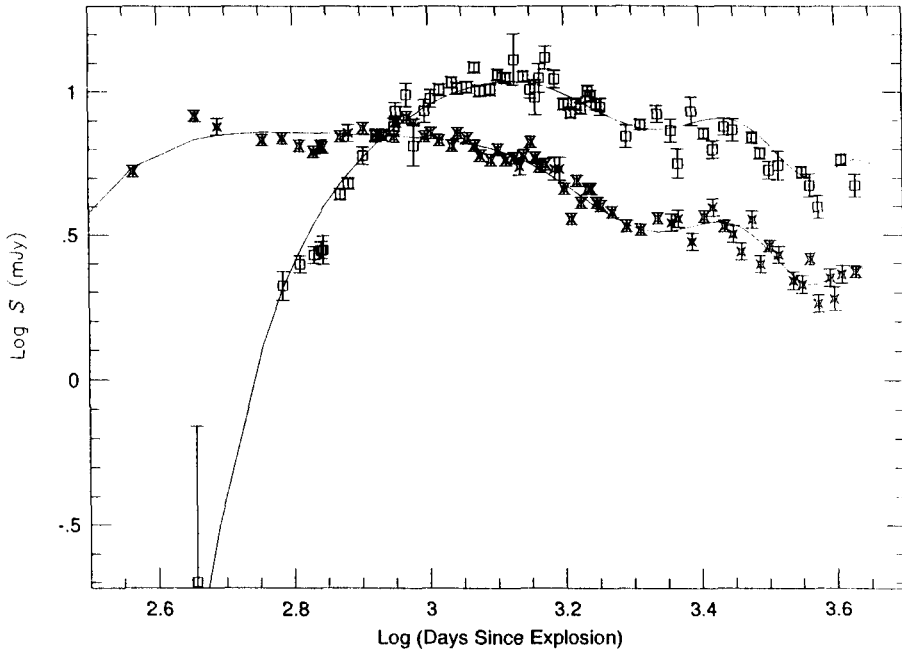


FIGURE 2. Radio light curves at 6 cm (stars) and 20 cm (squares) wavelength for the Type II “normal” supernova SN1979C in NGC4321 (M100) (From Weiler et al. 1992b).

3.3. SN1979C

3.3.1. Radio Light Curves

In April 1980 observation of the optical position of SN1979C in NGC4321 (M100) showed a bright, unresolved radio source where a year earlier no emission had been detectable. For this supernova the radio data are quite detailed with observations made on an average of once per month from 1980 to 1983 (usually at 20 and 6 cm wavelengths with occasional results at 2 cm) and measurements of ~ 4 times per year since 1984. The radio light curves and spectral index evolution have thus been firmly established and these are shown in Figures 2 and 3. Comparison of Figure 2 with Figure 1 shows that Type II RSNe turn on and off much more slowly in the radio than Type Ib/c’s.

SN1979C was identified as a Type II-L supernova and these radio light curves are thought to be typical of the class of “normal” Type II RSNe. The radio emission appears at 6 cm significantly after the optical outburst; there is an initial fast rise of the flux density; the emission brightens first at high frequencies and later at progressively lower frequencies; after the initial sharp rise, the flux density decays slowly over a period of months or years; and after the emitting region becomes optically thin, the radio spectral index is constant and reasonably typical for a non-thermal synchrotron source ($S \propto \nu^{-0.7}$). The early light curves are given by Weiler et al. (1986) and they have been extended by Weiler et al. (1991, 1992b).

3.3.2. Radio Light Curve Variations

In the process of analyzing a full decade of radio measurements from SN 1979C, Weiler et al. (1992b) found evidence for a significant, quasi-periodic, variation in the amplitude of the radio emission at 6 cm and 20 cm wavelengths of $\sim 15\%$ with a period of 1575 days or ~ 4.3 years (see Figure 2). They interpreted the variation as due to a minor ($\sim 8\%$)

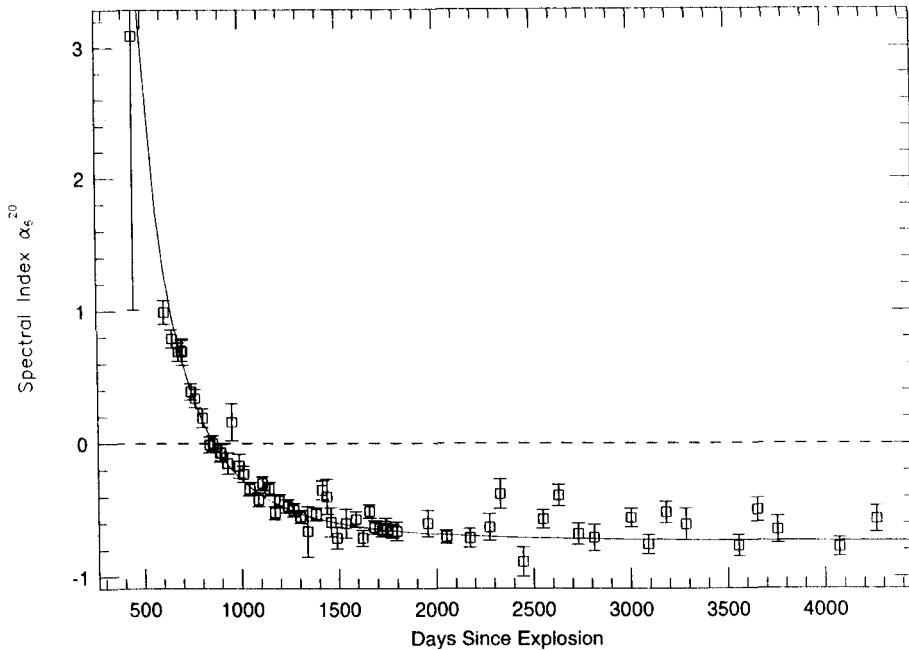


FIGURE 3. Spectral index α ($S \propto \nu^{+\alpha}$) evolution for SN1979C between 20 and 6 cm (from Weiler et al. 1991).

density modulation on the larger, relatively constant presupernova stellar mass loss rate (see model discussions in Section 5) with a period of ~ 4000 years. Since such a long period is inconsistent with most models for stellar pulsations, they concluded that, while thermal pulses and C/He flashes remain a possibility, the modulation may be produced by interaction of a binary companion in an eccentric orbit with the stellar wind from the presupernova RSG.

3.3.3. VLBI Measurements

The radio flux density of SN1979C has remained sufficiently high that Very Long Baseline Interferometry (VLBI) measurements have been carried out to establish its structure on the milliarcsecond scale. Bartel et al. (1985) have not only been able to measure the diameter of the radio source but, with successive observations, to show that it is clearly expanding. At 6 cm wavelength the diameter increased from 1.05 milliarcseconds in December 1982 to 1.43 milliarcseconds in December 1983. This rate, combined with the physical expansion velocity inferred from optical line velocity measurements of the SN photosphere, can be used to give an independent estimate of the distance to NGC4321 and of the Hubble Constant H_0 (Bartel et al. 1985). These results have been extended and improved by Bartel (1991a,b). While still not highly accurate, the technique shows promise to provide independent distance and Hubble Constant estimates, particularly for the recent SN1993J where the data is expected to be far superior.

3.4. *Mkn297A*

Radio studies of the galaxy Markarian 297 (NGC6052) by Yin & Heeschen (1991) show a compact radio source which, while not optically identified at the time of its outburst, shows turn-on, turn-off, and radio spectral properties very similar to those observed for RSNs. More recent studies (Yin 1994) appear to confirm this identification and show that

the flux density of the source, designated Mkn297A, has continued to evolve in a manner consistent with an RSN interpretation. The best fit modelling (Yin 1994) implies that Mkn297A exploded on approximately 1979 August 16 and has properties which resemble other RSNs such as SN1979C and SN1986J. Mkn297A appears to be the most luminous RSN ever observed. Unfortunately, Yin (1994) does not allow for the possible presence of mixed, internal, thermal absorbing/non-thermal emitting material (see Section 5) such as found for SN1986J (Weiler et al. 1986) and SN1988Z (Van Dyk et al 1993b) so that a more detailed comparison with possible subtypes cannot be carried out at present.

3.5. *SN1980K*

Only a few months after the radio detection of SN1979C, a new, bright Type II-L supernova, SN1980K, was discovered in NGC6946 in October 1980. Unlike SN1979C which was undetectable at 6 cm for a year, SN1980K could already be detected after a few weeks and the first detection of 0.7 mJy at 6 cm was obtained with the VLA on 4 December 1980. This early detection implies a lower mass loss rate from the progenitor star (see discussion in Section 6. Otherwise, the radio behavior of SN1980K was very similar to that of SN1979C and can be described by the same models. The available data and applicable models are described in detail by Weiler et al. (1986).

3.6. *SN1981K*

At a position where there had been no source detectable in Westerbork Synthesis Radio Telescope (WSRT) maps of NGC4258 made in the late 1970s, a January 1982 VLA map at 20 cm showed a strong point source (van der Hulst et al. 1983). Radio monitoring with the VLA and WSRT showed it to have a non-thermal spectrum and to be decreasing in flux density. A search of optical photographic plates revealed a transient object within 2 arcseconds of the radio position which had to have appeared near the beginning of August 1981. Although the scant optical data does not allow a determination of the type of this supernova, the slow radio decline implies that it was probably a Type II very similar in properties to SN1979C and SN1980K. SN1981K was apparently missed by optical searchers because it was likely quite faint ($\sim 16^m - 17^m$) and was at its optical brightest when NGC4258 was an early evening object. The radio results for SN1981K are discussed in more detail in Van Dyk et al. (1992).

3.7. *SN1986J*

3.7.1. *Radio Light Curves*

In a fashion similar to the discovery of SN1981K, VLA radio maps made of NGC891 at 20 cm in August 1986 showed a new, dominant point source ~ 65 arc-seconds south of the Galactic nucleus where no such object was detectable in earlier WSRT images (Rupen et al. 1987). This object, which received the designation SN1986J, is both one of the brightest (its 6 cm flux density has exceeded 100 mJy) and most radio luminous RSNs known (exceeded only by Mkn297A and SN1988Z).

After radio discovery, an optical counterpart was found for SN1986J in September 1986. Its luminosity in R band ($\lambda 6500 \text{ \AA}$) at that time was $\sim 19.5^m$ and examination of earlier observations of NGC891 made in January 1984 showed an ~ 18.4 magnitude object, also at R-band. The optical supernova showed a "peculiar" spectrum with narrow lines only $\sim 1000 \text{ km s}^{-1}$ wide while most SNe show line widths of at least several thousand kilometers per second.

The radio light curves for SN1986J through the end of 1988 are shown in Figure 4. Comparison of Figure 4 with Figure 2 shows that SN1986J was much slower in its turn-on than SN1979C, even though both were Type II RSNs. This is interpreted by

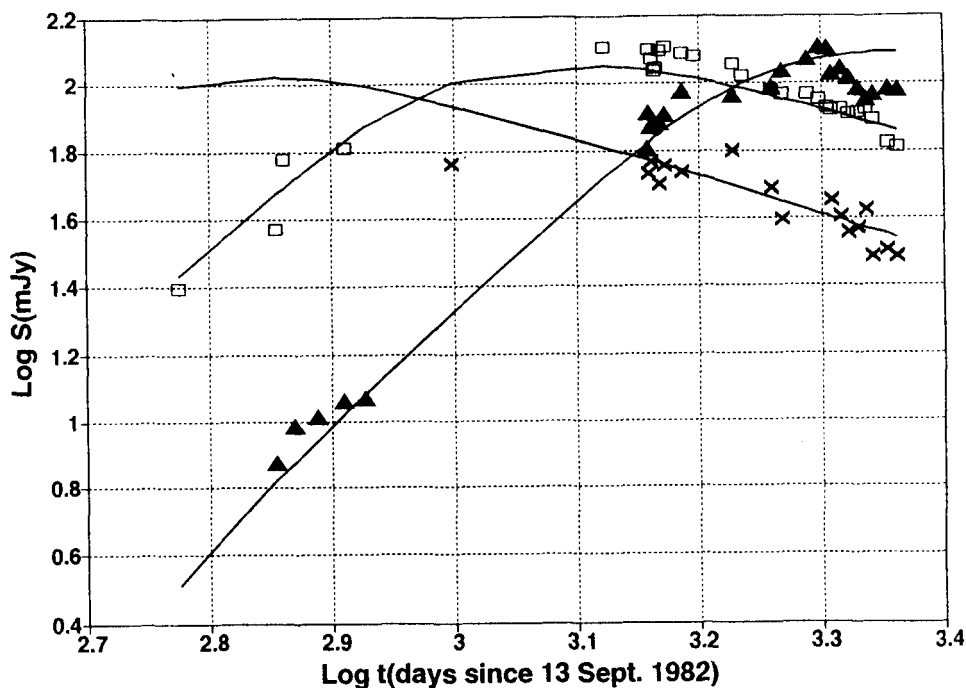


FIGURE 4. Radio light curves at 2 cm (crosses), 6 cm (squares), and 20 cm (triangles) for the Type II “peculiar” supernova SN1986J in NGC891. The age of the supernova is measured in days from the best fit date of explosion on 1982 September 13 (Weiler et al. 1990).

Weiler et al. (1990) as due to a much larger internal, thermal absorbing/non-thermal emitting component in the radio radiation for SN1986J than for SN1979C. Whether the presence of such internal material and its effect on the radio light curves is a fundamental difference between Type II “normal” RSNe such as SN1979C and SN1980K, with less evidence for an internal emitting/absorbing component, and Type II “peculiar” RSNe such as SN1986J and SN1988Z with strong evidence for such an internal component, or just a matter of degree is still not certain at present.

3.7.2. VLBI Structure

Because of its high apparent radio brightness, SN1986J is the only other RSN besides SN1979C which could be studied with VLBI before SN1993J. Initial measurements showed a radio diameter for SN1986J of ~ 0.0014 arc-seconds (Bartel et al. 1987, 1989) and, more recently, Bartel (1991b) has been able to obtain an actual VLBI map of SN1986J. It shows a shell-like structure, but is highly irregular with apparent extensions or lobes protruding beyond the shell. Because of this asphericity, SN1986J will not likely provide a very good target for distance or H_0 determinations.

3.8. SN1987A

Radio emission was detected from SN1987A already with the first observations made at 0.843 and 1.4 GHz only two days after discovery (Turtle et al. 1987). Observations one day later at 2.3 GHz also detected the supernova but with a flux density which was already declining rapidly. Although the peak radio flux density of SN1987A was >100 mJy, the Magellanic Clouds are so close that this implies an under-luminosity of a factor of more than 3 orders-of-magnitude when compared to, for example, SN1979C. Also, the radio emission from SN1987A declined extraordinarily rapidly and, except at 0.843 GHz,

was undetectably weak within a few days. With such a low radio luminosity and such rapid evolution, SN1987A would almost certainly not have been detected in the radio had it been at a more normal distance for extragalactic SNe such as the Virgo Cluster or even the Local Group during its initial evolution.

In retrospect, the origin of SN1987A in the explosion of a B3 Ia blue supergiant star agrees well with the observed radio properties. Such a star is not expected to have the massive stellar wind and dense circumstellar material produced prior to explosion needed to create a powerful RSN in mini-shell models (Weiler et al. 1986, Storey & Manchester 1987, Chevalier & Fransson 1987).

Recently, Staveley-Smith et al. (1992) have reported that SN1987A has again become detectable as a radio source, presumably due to the shock wave reaching denser material at the blue supergiant wind termination shock. Because of the likely asymmetry of the material (Ball & Kirk 1992) and the fact that the circumstellar material is already completely optically thin to radio emission, the turn-on characteristics and physical interpretation of the returning radio radiation is very different from that for the RSNs we are concerned with here.

3.9. SN1988Z

With a redshift of $z = 0.022$, SN1988Z in MCG +03–28–022 is the farthest RSN known with a distance of 89 Mpc ($H_0 = 75 \text{ km s}^{-1} \text{ Mpc}^{-1}$). It is also, after Mkn297A, the most luminous RSN known. Radio emission was first detected by Sramek, Weiler, & Panagia (1990) and further study of its radio emission and model fitting to the results by Van Dyk et al. (1993b) indicate that it has properties which are very similar to those of SN1986J. It is thus apparently an example of a Type II “peculiar” RSN like SN1986J which shows the slow radio light curve turn-on which is characteristic of the presence of a significant component of mixed, internal thermal absorbing/non-thermal emitting material in the SN shock interaction region. Unfortunately, because of its great distance it is relatively weak with a maximum flux density at 6 cm of $< 2 \text{ mJy}$, making it very hard to study with high accuracy. Nevertheless, Van Dyk et al. (1993b) have extensive measurements at four radio frequency bands.

3.10. SN1993J

SN1993J was discovered by the Spanish amateur astronomer F. Garcia on 1993 March 26.9 UT in M81 (Ripero 1993) and first detected in the radio at 1.3 cm on 1993 April 2 by Weiler et al. (1993). Since that time extensive monitoring has been carried out by various observers and detections have been obtained at all frequencies from 1.4 GHz to 100 GHz. The behavior of SN1993J in the radio range is apparently rather normal, resembling the evolution of SN1979C and SN1980K. However, the modelling of the preliminary light curves, which is still incomplete, does require a small, but significant internal, thermal absorbing/non-thermal emitting component such as was required for SN1986J. These observations and our preliminary modelling results are discussed further by Van Dyk et al. (1993) in the workshop on SN1993J included as part of this volume.

4. Intermediate Age Radio Supernovae

Monitoring of recent RSNs has shown that centimeter radio emission from Type II SNe can last for several years. Studies of young SNRs such as Cas A (SN 1670) and SNR models (see, e.g., Gull 1973) show that after ~ 100 years SNRs can become powerful radio sources. However, the question remains as to what the radio properties of SNe and SNRs are in the time interval from $10 < t(\text{yrs}) < 300$, the so-called intermediate age SNe.

There is at least a partial answer in the detection of radio emission from SN1957D and, perhaps, SN1950B in M83 (NGC5236) (Cowan & Branch, 1985). The 6 cm luminosity of SN1950B is about 5 times that of Cas A and SN1957D is about 15 times Cas A (Weiler et al. 1986). The optical classifications of these two SNe are unknown, but the radio properties resemble the Type II supernovae SN1979C and SN1980K.

A radio source coincident to better than 0.1 arcseconds with the position of SN1961V was detected with the VLA at 20 cm (Branch & Cowan 1985; Klemola 1986). This source is very weak, 0.19 mJy, which, at the distance of M83, implies an absolute luminosity about equal to that of Cas A. More recent observations of this source at 6 cm (Cowan et al. 1988) show it to have a nonthermal spectrum with index $\alpha \sim -0.4$. Since the supernova is embedded in an HII region some portion of the radio emission may be thermal although the thermal contribution is not thought to be significant (Cowan et al. 1988). SN1961V is particularly interesting because it was considered to be the prototype of the Zwicky Type V supernova, with an optical spectrum like a Type II object but with relatively narrow lines corresponding to an expansion velocity of only $\sim 2000 \text{ km s}^{-1}$ and a very slowly declining optical light curve. Recently, however, Goodrich, Stringfellow, & Penrod (1989) and Bower et al. (1993) postulate that SN1961V was not a true supernova but an exaggerated η Carinae-type outburst. years.

It is not yet known if the radio sources related to SN1961V, SN1957D, and SN1950B are old RSNe which are slowly declining or young SNR which are brightening as they sweep up interstellar matter. Continued monitoring of the sources should answer this question within the next several years.

5. Models for Radio Supernovae

In their study of a number of RSNe Weiler et al. (1986) established several identifying properties:

- (a) non-thermal emission with high brightness temperature;
- (b) turn-on first at shorter wavelengths and later at longer wavelengths;
- (c) initial rapid increase of flux density with time at each wavelength;
- (d) power law decline in flux density at each wavelength after maximum is reached;
- (e) initial decrease in spectral index α between any two wavelengths as the longer wavelength goes from optically thick to optically thin, and a final asymptotic approach of the spectral index to an optically thin, non-thermal, constant negative value ($S \propto \nu^{+\alpha}$).

Models for RSNe have to describe the origin and evolution of the relativistic particles and magnetic fields which give rise to these properties. Two classes of models have been developed to describe the radio emission from SNe (see Weiler et al. 1986), the “mini-shell” (Chevalier 1982, 1984) model which utilizes shock acceleration in the region exterior to the supernova ejecta and the “mini-plerion” (Pacini & Salvati 1981) model which utilizes the rotational energy losses of a rapidly spinning, rapidly slowing pulsar left over by the SN explosion. However, all presently available data appear to be best described by the “mini-shell” model.

The mini-shell model utilizes the Rayleigh-Taylor unstable region between the supernova shock, propagating into the preexisting circumstellar shell of dense material which was created by a stellar wind from the presupernova star and the reverse shock propagating back into the supernova envelope to drive turbulence. This results in the magnetic field enhancement and particle acceleration necessary for radio synchrotron radiation (Chevalier 1984). Since the circumstellar shell is ionized and generally optically thick at radio frequencies, emission does not become observable until the shock wave has passed far enough through the shell that the radio optical depth approaches unity. The change

in the remaining optical depth then produces the observed rapid turn on at progressively lower frequencies and the density gradient of the supernova envelope provides a declining radio light curve of the form $S \propto \nu^\alpha t^\beta$ similar to that observed. Both the intensity and the time scale of the radio emission are dependent on the characteristics of the circumstellar material and are thus an indication of the mass loss rate of the supernova progenitor. Adopting a model with an external thermal, absorbing screen of optical depth τ and an internal, mixed, thermal absorbing/non-thermal emitting medium of optical depth τ' , and ruling out such absorbing processes as synchrotron self-absorption and the Razin-Tsytoich effect, the radio “light curves” of the RSNs can be described with the simple mathematical form:

$$S(\text{mJy}) = K_1 \left(\frac{\nu}{5 \text{ GHz}} \right)^\alpha \left(\frac{t - t_0}{1 \text{ day}} \right)^\beta e^{-\tau} (1 - e^{-\tau}) \tau'^{-1}, \quad (5.1)$$

with

$$\tau = K_2 \left(\frac{\nu}{5 \text{ GHz}} \right)^{-2.1} \left(\frac{t - t_0}{1 \text{ day}} \right)^\delta, \quad (5.2)$$

and

$$\tau' = K_3 \left(\frac{\nu}{5 \text{ GHz}} \right)^{-2.1} \left(\frac{t - t_0}{1 \text{ day}} \right)^\delta, \quad (5.3)$$

This formulation assumes that the flux density S , the external optical depth τ , and the internal optical depth τ' are well described by power-law functions of the supernova age $(t - t_0)$, with powers β , δ , and δ' , respectively; that the external absorption τ is purely thermal, free-free absorption in an ionized medium (frequency dependence $\nu^{-2.1}$) with a radial dependence of r^{-2} from a constant speed, red supergiant wind; that the internal absorption τ' is also thermal but mixed, at least statistically, with the non-thermal emitting medium; and that the intrinsic emission is due to the nonthermal synchrotron process with an optically thin spectral index α . The quantities K_1 , K_2 , and K_3 are three scaling factors for the units of choice of mJy, GHz, and days, and correspond formally to the flux density (K_1), external optical depth (K_2), and internal optical depth (K_3) at 5 GHz 1 day after the SN explosion.

This simple model has proven to be very satisfactory for all known RSNs either of Type II or Type Ib/c. To limit the number of free parameters, we adopt the Chevalier (1981, 1982) model which determines $\delta \equiv \alpha - \beta - 3$. We also adopt a modification of the Chevalier model proposed by Weiler et al. (1990) which fixes $\delta' \equiv 5\delta/3$. It has been noted by Weiler et al. (1990) that the mixing of the thermal absorbing/ non-thermal emitting material is a mixing in a statistical sense, which probably does not involve physical admixture of the two media. The need for such a component is likely evidence for the presence of blobs, filaments, lobes, or other asymmetric structures of thermal material throughout the non-thermal emitting region.

All fits of the data to equations 5.1 – 5.3 are carried out by searching parameter space for a minimum χ^2 and generally yield quite satisfactory descriptions of the RSN radio light curves.

TABLE 2. Parameters for Well Studied RSNs

SN	K_1	α	β	K_2	K_3	m	n	\dot{M}
Type Ib/c SNe								
1983N	4.4×10^3	-1.03	-1.59	5.3×10^2		0.81	7	8.0×10^{-6}
1984L	2.8×10^2	-1.01	-1.48	6.9×10^2		0.84	8	7.3×10^{-6}
1990B	2.0×10^2	-1.12	-1.27	1.5×10^4		0.95	> 20	1.5×10^{-5}
Type II SNe								
1979C	1.5×10^3	-0.74	-0.78	3.7×10^7		0.99	> 20	5.9×10^{-4}
1980K	7.4×10^1	-0.52	-0.66	3.4×10^5		0.95	> 20	7.2×10^{-5}
1981K	1.9×10^1	-0.74	-0.50	$< 1.5 \times 10^5$		1.08	> 20	1.9×10^{-5}
1986J	6.7×10^5	-0.67	-1.18	3.0×10^5	4.0×10^{12}	0.83	8	1.7×10^{-4}
1988Z	1.5×10^5	-0.80	-1.50	5.8×10^4	1.0×10^{12}	0.77	6	1.2×10^{-4}

6. RSN Model Parameters and Mass Loss Rates

Through the use of the Chevalier model, it is possible to probe the physics of the RSN phenomenon and the presupernova stellar systems. The parameter α is the spectral index of the non-thermal emission and is directly related to the relativistic electron energy distribution index γ ($N(E) \propto E^{-\gamma}$) by $\gamma = -2\alpha + 1$. This electron energy distribution index γ and the index m of the expansion rate of the interaction shell radius R ($R \propto t^m$) are related to the rate of decline of the non-thermal emission β by $\beta = -(\gamma + 5 - 6m)/2$. The index of the expansion rate of the interaction shell m also determines the temporal behavior of the external ($\delta = -3m$) and mixed ($\delta' = 5\delta/3 = -5m$) thermal absorbing material. Under the Chevalier model, the parameter m is also related to the gas density ρ in the outer parts of the supernova ($\rho \propto r^{-n}$ where $m = (n - 3)/(n - 2)$). Finally, the Chevalier model allows an estimation of the mass loss rate in $M_{\odot} \text{ yr}^{-1}$ from the presupernova stellar system. Using the formulation given by Weiler et al. (1986) in their Equation 16 and the assumptions:

- (a) presupernova RSG wind velocity $w = 10 \text{ km s}^{-1}$,
- (b) initial supernova ejecta velocity $v_i = 1.5 \times 10^4 \text{ km s}^{-1}$,
- (c) electron temperature in the RSG wind $T = 10^5 \text{ K}$

and the other assumptions listed by Weiler et al. (1986), we can estimate presupernova mass loss rates.

For those RSNs where sufficient data exist to obtain satisfactory fits, the best value estimates for the model parameters are listed in Table 2. Note that in many cases the estimated mass loss rates are approximately an order of magnitude larger than previously given values in the literature. While more data and better model fits have altered parameter values slightly for a few of the RSNs, most of the change results from an assumption of a higher electron temperature in the RSG wind ($T \simeq 10^5 \text{ K}$ vs. $T \simeq 10^4 \text{ K}$ previously) and a higher estimated ejecta velocity ($v_i \simeq 1.5 \times 10^4 \text{ km s}^{-1}$ vs. $v_i \simeq 10^4 \text{ km s}^{-1}$ previously).

7. RSN Results

7.1. Classifications

Now that more than a dozen RSNs are known and more than a half dozen are well studied, it is possible to draw a number of conclusions from examining their similarities and differences. For example, Type Ib/c supernovae appear to have steeper spectral indices (α) than Type II supernovae. Examination of Table 2 shows that the spectral index demarcation is at approximately $\alpha = -0.9$ with the Type Ib/c RSNs being steeper and the Type II RSNs being flatter. Additionally, the Type Ib/c RSNs appear to be fairly similar objects in decline rate (β) while the Type II RSNs appear to split into two groups, those like the “normal” RSN SN1979C (SN1979C, SN1980K, SN1981K) and those like the “peculiar” RSN SN1986J (SN1986J, SN1988Z). The former group appears to decline more slowly (β flatter) than the latter group (β steeper) with the SN1986J-like RSNs having decline rates quite similar to Type Ib/c RSNs. The external absorption (K_2) is lower for Type Ib/c RSNs than for Type II’s and the internal absorption (K_3) is small to negligible for all RSNs except for the SN1986J-like. Correspondingly, the presupernova mass loss rates (\dot{M} in $M_{\odot} \text{ yr}^{-1}$) for Type Ib/c RSNs are always lower than those for Type II’s. The amount of deceleration of the ejecta is more significant (m smaller) for Type Ib/c RSNs than for the SN1979C-like RSNs which indicates a correspondingly much steeper density gradient (n) in the ejecta for the latter. Interestingly enough, the SN1986J-like RSNs have values for m and n which are very similar to those found for Type Ib/c RSNs. The unusually high value of m and n for SN1990B may not be significant, since the SN was very weak in the radio and the data had large errors.

In general, it appears that Type Ib/c RSNs are clearly distinguishable in their radio emission from Type II RSNs. Also, it appears that Type II RSNs split into two distinguishable groupings based on their radio emission, as is also apparent in their optical emission (see the discussion of SN1986J above). Whether this bifurcation of Type II radio properties is an indication of clear physical differences between the two types of SNe or simply a matter of degree, such as mass of the presupernova star, is not clear at present. More examples of Type II RSNs will have to be studied.

7.2. Luminosity vs. Time delay

According to the Chevalier model, both the radio emission and the initial absorption for a supernova are a function of the mass lost from the presupernova star in a dense stellar wind prior to explosion. As a preliminary investigation of this, we have plotted in Figure 5 the peak observed 6 cm luminosity against the number of days required from explosion to reach that peak. Although the interpretation of this is still preliminary, examination of Figure 5 indicates two possible correlations:

(a) Type Ib/c RSNs are quite similar in their maximum 6 cm spectral luminosities and may represent standard radio candles;

(b) Type II RSNs, if they do not bifurcate into two groupings as discussed above, may have a direct relation between the maximum 6 cm spectral luminosity and the time after explosion required to reach that maximum.

In particular, the present data are consistent with a relation of the form

$$L_{6\text{cm max}} = 1.6 \times 10^{22} (t_{6\text{cm max}} - t_0)^{1.90}. \quad (7.4)$$

with L in $\text{erg s}^{-1} \text{ Hz}^{-1}$ and t in days. If such a relation can be strengthened by further observational data, then the Type II RSNs could also be calibrated to yield distance information since direct measurement of the observed turn-on time at 6 cm would indicate the absolute radio spectral luminosity.

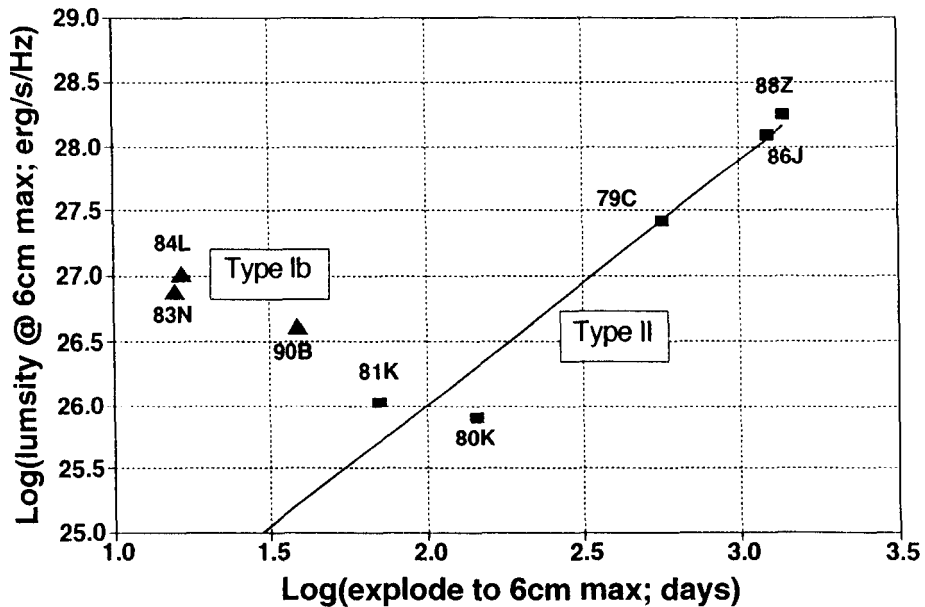


FIGURE 5. Radio peak 6 cm spectral luminosity *vs.* time from explosion to 6 cm maximum flux density.

It must be kept in mind, however, that such relations as proposed here are highly speculative and still must be demonstrated with more certainty.

8. Summary

Although the radio supernova phenomenon is relatively new, having been developed essentially in its entirety since the detection of SN1979C at 6 cm in April 1980, its study has met with considerable success. Detailed multiwavelength radio light curves have been obtained for a number of supernovae; the number of high quality upper limits on other supernovae has been increased significantly; and theoretical interpretation of the phenomenon has developed well. The gross structures of the radio light curves have been determined and can be related to the properties of the supernova's progenitor stellar system, its immediate environment, and its likely state in the last stages of evolution before exploding. As the numbers of well studied examples increases, systematic trends are appearing and the description of presupernova stellar systems based on their radio behavior after explosion is improving rapidly. There is even the speculative possibility that RSNe can serve as independent distance calibrators. Observations are continuing on already known RSNe and new, bright supernovae are being studied with the VLA as they occur. The recent explosion of the close, optical and radio bright SN1993J promises to extend our understanding of these unusual objects even further.

REFERENCES

- Allen, R.J., Goss, W.M., Ekers, R.D., & de Bruyn, A.G. 1976, *A&A*, 48, 253
 Ball, L., & Kirk, J.G. 1992, *ApJ*, 396, L39
 Bartel, N. 1991a, in *The 10th Santa Cruz Workshop in Astronomy & Astrophysics*, ed. S.E. Woosley (Springer Verlag), p. 760

- Bartel, N. 1991b, in *The 10th Santa Cruz Workshop in Astronomy & Astrophysics*, ed. S.E. Woosley (Springer Verlag), p. 503
- Bartel, N., Rogers, A.E.E., Shapiro, I.I., Gorenstein, M.V., Gwinn, C.R., Marcaide, J.M., & Weiler, K.W. 1985, *Nature*, 318, 25
- Bartel, N., Rupen, M.P., & Shapiro, I.I. 1987, *IAU Circ. No. 4292*
- Bartel, N., Rupen, M.R., & Shapiro, I.I. 1989, *ApJ*, 337, L85
- Bower, G.C., Filippenko, A.V., Ho, L.C., Stringfellow, G.S., Goodrich, R.W., & Porter, A.C. 1993, *BAAS*, 25, 819
- Branch, D., & Cowan, J.J. 1985, *ApJ*, 297, L33
- Chevalier, R.A. 1981, *ApJ*, 251, 259
- Chevalier, R.A. 1982, *ApJ*, 259, 302
- Chevalier, R.A. 1984, *Ann. N. Y. Acad. Sci.*, 422, 215
- Chevalier, R.A., & Fransson, C. 1987, *Nature*, 328, 44
- Cowan, J.J., & Branch, D. 1982, *ApJ*, 258, 31
- Cowan, J.J., & Branch, D. 1985, *ApJ*, 293, 400
- Cowan, J.J., Henry R.B.C., & Branch, D. 1988, *ApJ*, 329, 116
- Cowan, J.J., Goss, W.M., & Sramek, R.A. 1991, *ApJ*, 379, L49
- Goodrich, R.W., Stringfellow, G.S., & Penrod, G.D. 1989, *ApJ*, 342, 908
- Gottesman, S.T., Broderick, J.J., Brown, R.L., Balick, B., & Palmer, P. 1972, *ApJ*, 174, 383
- Gull, S.F. 1973, *MNRAS*, 161, 47
- Klemola, A.R. 1986, *PASP*, 98, 464
- Kronberg, P.P., & Sramek, R.A. 1985, *Science*, 227, 28
- Pacini, F., & Salvati, M. 1981, *ApJ*, 245, L107
- Panagia et al. 1980, *MNRAS*, 192, 861 (Table 1, Ref. 6)
- Panagia, N., Sramek, R.A., & Weiler, K.W. 1986, *ApJ*, 300, L55 (Table 1, Ref. 3)
- Ripero, J. 1993, *IAU Circ. No. 5731*
- Rupen, M.P., van Gorkom, J.H., Knapp, G.R., Gunn, J.E., & Schneider, D.P. 1987, *AJ*, 94, 61
- Ryder, S., Staveley-Smith, L., Dopita, M., Petre, R., Colbert, E., Malin, D., & Schlegel, E. 1993, *ApJ*, in press (Table 1, Ref. 5)
- Sramek, R.A., & Weiler, K.W. 1990, in *Supernovae*, ed. A.G. Petschek (Springer Verlag), 76
- Sramek, R.A., Weiler, K.W., & Panagia, N. 1990 *IAU Circ. No. 5112*
- Sramek, R.A., Panagia, N., & Weiler, K.W. 1984, *ApJ*, 285, L59 (Table 1, Ref. 1)
- Staveley-Smith, L., Manchester, R.N., Kesteven, M.J., Campbell-Wilson, D., Crawford, D.F., Turtle, A.J., Reynolds, J.E., Tzioumis, A.K., Killeen, N.E.B., & Jauncey, D.L. 1992, *Nature*, 355, 147 (Table 1, Ref. 16)
- Storey, M.C., & Manchester, R.N. 1987, *Nature*, 329, 421 (Table 1, Ref. 17)
- Turtle, A.J., Campbell-Wilson, D., Bunton, J.D., Jauncey, D.L., Kesteven, M.J., Manchester, R.N., Norris, R.P., Storey, M.C., & Reynolds, J.E. 1987, *Nature*, 327, 38 (Table 1, Ref. 15)
- van der Hulst, J.M., Hummel, F., Davies, R.D., Pedlar, A., & van Albada, G.D. 1983, *Nature*, 306, 566
- Van Dyk, S.D., Weiler, K.W., Sramek, R.A., & Panagia, N. 1992, *ApJ*, 396, 195 (Table 1, Ref. 13)
- Van Dyk, S.D., Sramek, R.A., Weiler, K.W., & Panagia, N. 1993a, *ApJ*, 409, 162 (Table 1, Ref. 4)
- Van Dyk, S.D., Weiler, K.W., Sramek, R.A., & Panagia, N. 1993b, *ApJL*, 419, L69 (Table 1, Ref. 18)
- Van Dyk, S.D., Weiler, K.W., Sramek, R.A., Rupen, M.P., & Panagia, N. 1993, contribution to the SN1993J Workshop in this volume (Table 1, Ref. 19)
- Weiler, K.W., & Sramek, R.A. 1988, *Ann. Rev. A&A*, 26, 295

- Weiler, K.W., van der Hulst, J.M., Sramek, R.A., & Panagia, N. 1981, *ApJ*, 243, L151 (Table 1, Ref. 7)
- Weiler, K.W., Sramek, R.A., Panagia, N., van der Hulst, J.M., & Salvati, M. 1986, *ApJ*, 301, 790 (Table 1, Ref. 2)
- Weiler, K.W., Panagia, N., Sramek, R.A., van der Hulst, J.M., Roberts, M.S., & Nguyen, L. 1989, *ApJ*, 336, 421
- Weiler, K.W., Panagia, N., & Sramek, R.A. 1990, *ApJ*, 364, 611 (Table 1, Ref. 14)
- Weiler, K.W., Van Dyk, S.D., Panagia, N., Sramek, R.A., & Discenna, J.L. 1991, *ApJ*, 380, 161 (Table 1, Ref. 8)
- Weiler, K.W. Van Dyk, S.D., Panagia, N., & Sramek, R.A. 1992a, *ApJ*, 398, 248 (Table 1, Ref. 12)
- Weiler, K.W. Van Dyk, S.D., Pringle, J.E., & Panagia, N. 1992b, *ApJ*, 399, 195 (Table 1, Ref. 9)
- Weiler, K.W. Sramek, R.A., Van Dyk, S.D., & Panagia, N. 1993, *IAU Circ. No. 5752*
- Yin, Q.F. 1994, *ApJ*, 420, 152 (Table 1, Ref. 11)
- Yin, Q.F., & Heeschen, D.S. 1991, *Nature*, 354, 130 (Table 1, Ref. 10)